Functional organic matter components in mangrove soils revealed by density fractionation

Running title: Density fractions of mangrove SOM

This is a non-peer reviewed preprint that has not been submitted to any journals.

Kota Hamada[1], Toshiyuki Ohtsuka[2], Nobuhide Fujitake[1], Toshihiro Miyajima[3], Yusuke Yokoyama[3,4,5,6,7], Yosuke Miyairi[3], Morimaru Kida [1]*

[1] Soil Science Laboratory, Graduate School of Agricultural Science, Kobe University, 1-1 Rokkodai, Nada, Kobe, Hyogo 657-8501, Japan

[2] River Basin Research Center, Gifu University, 1 Yanagito, Gifu, Gifu 501-1193, Japan

[3] Atmosphere and Ocean Research Institute, The University of Tokyo, 5-1-5 Kashiwanoha, Kashiwa, Chiba 277-8564, Japan

[4] Department of Earth and Planetary Science, Graduate School of Science, The University of Tokyo, 7-3-1 Hongo, Bunkyo, Tokyo 113-0033, Japan

[5] Graduate Program on Environmental Sciences, The University of Tokyo, 3-8-1 Komaba, Meguro, Tokyo 153-8902, Japan

[6] Department of Biogeochemistry, Japan Agency for Marine-Earth Science and Technology, 2-15 Natsushima, Yokosuka, Kanagawa 237-0061, Japan

[7] Research School of Physics, The Australian National University, Canberra, ACT0200, Australia

* Corresponding author e-mail: morimaru.kida@people.kobe-u.ac.jp

ORCID ID: 0000-0002-9908-2012 (Morimaru Kida)

Abstract

The mechanisms underlying stabilization of soil organic matter (SOM) in coastal ecosystems, including mangrove forests, are poorly understood, limiting our ability to predict the consequences of disturbances. Here, we introduce density fractionation to mangrove soils to identify the distribution and properties of the functional components of SOM with regard to degradation state, stability, and origin, namely, the high-density fraction (HF), free low-density fraction (f-LF), and mineral-associated LF (m-LF). Three soil cores (1 m) were collected in a mangrove forest on Ishigaki Island, Japan and cut into 10 cm intervals and analyzed. The massive production of mangrove fine roots resulted in a high abundance of LFs throughout the cores, which markedly differed from terrestrial soils. Relative abundance of LFs together accounted for 38%–66% of total soil C. The m-LF was as abundant as f-LF and 1.6 times higher in relative abundance than the global average of terrestrial soils. The C/N ratios and $\delta^{13}C$ values clearly increased with depth in all fractions, which was attributed to the increased contribution from roots. We found a consistent pattern in $\Delta^{14}C$ values of density fractions. HF was the oldest with $\Delta^{14}C$ between -149‰ and -97‰ followed by m-LF (between -130‰ and -87‰) and then f-LF (between -89‰ and 78‰), suggesting that mineral association may be pivotal in long-term carbon storage in the mangrove mineral soil. Our analysis successfully identified meaningful functional components of mangrove SOM, yet several questions remained unanswered, including large

variability in $\Delta^{14}C$ in different cores. Future studies would benefit from a coupled analysis of the quantity and quality of density fractions and geochemical factors in the mangrove soil.

Keywords: Blue carbon; Coastal vegetated ecosystem; Persistence; Physico-chemical protection; Radiocarbon

1. Introduction

Coastal ecosystems such as mangrove forests exhibit a high capacity for soil organic matter (SOM) storage (Bouillon, Borges, *et al.*, 2008; Kristensen *et al.*, 2008). The global average carbon stock in the top 1 m of mangrove forest soils is estimated to be 283 ± 193 Mg C ha^{-1} (Atwood *et al.*, 2017). Furthermore, regardless of the soil type (i.e., peaty or mineral), the average carbon stock including deeper soils (~3 m) exceeds 900 Mg C ha^{-1}, making mangrove forests among the most carbon-rich ecosystems in the tropics (Donato *et al.*, 2011; Kida *et al.*, 2021). Coastal vegetated ecosystems, known as "Blue Carbon" ecosystems, including mangrove forests, are known to accumulate SOM at rates tens of times faster than terrestrial ecosystems (McLeod *et al.*, 2011), with SOM accounting for about 75% of total carbon stocks in mangrove forests (Alongi, 2014). Ongoing climate change and anthropogenic disturbances such as deforestation, land reclamation, urbanization, and land use change pose significant threats to these ecosystems (Adame *et al.*, 2021; Richards and Friess, 2016). These disturbances can significantly impact carbon sequestration in coastal ecosystems and existing soil carbon pools. However, the mechanisms of SOM stabilization in these ecosystems are poorly understood, limiting our ability to predict the consequences of disturbances (Kida and Fujitake, 2020).

Some stabilization mechanisms must be present for mangrove SOM to remain stable over the long-term. However, research on this topic is still scarce for mangrove soils and Blue

Carbon ecosystems in general. While Blue Carbon studies have gathered significant information on the global C stocks and their regional variations in the last decade, a mechanistic understanding of SOM stabilization in these systems has been comparatively much less developed (Kida and Fujitake, 2020). Anoxia has been considered a dominant factor in SOM stabilization in these coastal vegetated ecosystems, as certain organic compounds, particularly lignin, are degraded less efficiently in the absence of oxygen, and it is most likely the primary reason behind the millennial-scale accumulation of mangrove peat on oceanic islands (McKee *et al.*, 2007). However, evidence is accumulating that SOM in mineral soils of coastal vegetated ecosystems consists of a myriad of different organic compounds (Dodla *et al.*, 2012; Kida *et al.*, 2019; Santín *et al.*, 2008; Zhang *et al.*, 2016). Previous studies have shown that labile organic components including many small organic compounds, tissues of micro autotrophs such as algae and phytoplankton, and fresh plant litter degrade at similar rates regardless of the presence or absence of oxygen (Lee, 1992). Therefore, factors contributing to the stabilization of these otherwise labile compounds in mangrove mineral soils are of particular interest.

Several common mechanisms underlying SOM stabilization have been identified in terrestrial soils and marine sediments. Broadly, these include: (1) recalcitrance of organic matter due to its chemical structural properties, (2) physical protection (inaccessibility) of organic matter from microbial degradation within aggregates and pore spaces, and (3) chemical interactions with

85 soil minerals and metals (Sollins *et al.*, 1996). The physical and chemical stabilization of SOM
86 reduces its availability to microorganisms and enzymes (Lützow *et al.*, 2006; Marschner *et al.*,
87 2008). Coastal vegetated soils, located in the transitional zone between terrestrial and marine
88 environments, may also experience the same mechanisms of SOM stabilization. However,
89 contrasting evidence has been found regarding the potential mechanisms that contribute to SOM
90 stabilization in these ecosystems (Table1). It is important to investigate whether physical and
91 chemical stabilization of potentially labile organic matter is also present in mangrove mineral
92 soils and coastal sediments, but few related studies have been conducted to date (Dicen *et al.*,
93 2019; Shields *et al.*, 2016; Zhao *et al.*, 2018).

94 Density fractionation, which has been used by soil scientists for nearly 50 years,
95 physically fractionates SOM into functional fractions of varying stability using a heavy liquid
96 based on particle density (Crow *et al.*, 2007). Chemical and molecular analysis of organic matter
97 after density fractionation allows for the acquisition of higher-resolution data about the
98 spatiotemporal distribution and properties of the functional components of SOM with regard to
99 stability and origin. The particle density of freshly incorporated, plant-derived particulate organic
100 matter is less than 1.6 g cm^{-3}, considerably smaller than that of soil minerals (2–4 g cm^{-3}). As a
101 result, density fractionation yields two fractions based on density: the low-density fraction (LF,
102 also known as particulate organic matter) and high-density fraction (HF, also known as mineral-

103 associated organic matter). The interaction between organic matter and minerals increases as the
104 microbial degradation of plant-derived LF progresses. LF can be further divided into free LF (f-
105 LF), a roughly mineral-free fraction consisting mainly of fresh, coarse organic materials such as
106 plant residues, and mineral-associated LF (m-LF) which is LF attached to or embedded in soil
107 minerals or aggregates, by disruption of soil aggregates and mineral association through
108 mechanical shaking with glass beads or ultrasonication (Wagai *et al.*, 2009). Conceptually, f-LF
109 is labile and fast-cycling due to the lack of protection by minerals, while HF is the most persistent,
110 cycled at centuries to millennium time-scale, due to physico-chemical protection by soil mineral
111 matrix, and m-LF often exhibits properties intermediate between the two (Wagai *et al.*, 2009).
112 Density fractionation thus physically divides bulk SOC into pools directly associated with specific
113 mechanisms and processes that affect its decomposition rate (Heckman *et al.*, 2022). While
114 density fractionation has been used in other coastal ecosystems such as seagrass meadows
115 (Miyajima *et al.*, 2017), it has not yet been applied to mangrove soils. Considering the massive
116 production and turnover of fine roots in mangroves soils and their major contribution to SOM
117 accumulation (Arnaud *et al.*, 2021; Liu *et al.*, 2017; Muhammad-Nor *et al.*, 2019) and recently
118 proposed possible roles of soil physico-chemical factors in stabilizing SOC in coastal vegetated
119 ecosystems (Dicen et al., 2019; Kida and Fujitake, 2020; Shields et al., 2016; Zhao et al., 2018),
120 density fractionation appears particularly useful in studying SOM stabilization mechanisms in

mangrove soils.

The aim of this study was to identify the quantitatively important fractions for carbon storage in mangrove soils using density fractionation, to examine the differences in organic matter characteristics by fraction and depth, and to estimate the origin of organic matter in each density fraction. Previous research has shown that approximately 80% of fine root biomass is found within the top 30 cm of terrestrial soils (Hashimoto and Hyakumachi, 1998), while in mangrove forests, fine root production is likely much greater and fine roots are widely distributed to deeper depth (Arnaud *et al.*, 2021; Tabuchi, 1983). Therefore, we hypothesized that f-LF is more abundant in mangrove soils compared to terrestrial soils. We also hypothesized that HF exhibits more non-mangrove (microbes or marine origin) signatures compared to other LFs because HF can capture other sources in water through organo-mineral interactions (Kida and Fujitake, 2020).

2. Materials and Methods

2.1. Study area and sampling

Samples were collected in a mangrove forest located along the Fukido River on Ishigaki Island, Okinawa Prefecture, Japan (24°29' N, 124°13' E, Fig. 1). This forest covers an area of approximately 19 ha around the mouth of the Fukido River, and are dominated by two mangrove species, *Bruguiera gymnorrhiza* and *Rhizophora stylosa*. The study area has a subtropical

139 monsoon climate, with an average annual precipitation of 2107 mm and an average annual
140 temperature of 24.3°C from 1981 to 2010 (Ishigakijima Island Local Meteorological Observatory,
141 Japan Meteorological Agency). The watershed (approximately 2.4 km^2) receives little human
142 activity, and broadleaf forests occupy about 95% of the area, with the rest of land use being sparse
143 sugar cane and paddy fields. The soil in the catchment is red-yellow soil (Oxisols) with a thin A
144 horizon and low SOM content. A previous study has detailed the species composition, biomass,
145 and aboveground net primary productivity of this mangrove forest (Ohtsuka *et al.*, 2019). The
146 Fukido mangrove exhibits a clear semidiurnal tide, with maximum tidal height reaching over 1 m
147 at spring tide (Ohtsuka *et al.*, 2019). At high tide, the area is inundated with seawater, whereas at
148 low tide, the soil surface is exposed to the air. The soil is mineral and tentatively classified as gley
149 soil. The mineral composition within the mangrove forest is spatially relatively constant, with
150 only a minimal contribution from calcite, indicating that the minerals were mainly derived from
151 the catchment (Kinjo *et al.*, 2005).

152 Soil samples were collected in August 2015 at five points within a permanent quadrat
153 (80 m × 80 m) established at the site in 2014 (Ohtsuka *et al.*, 2019) using an open-face stainless
154 core sampler with minimum compaction (1 m long, 27 cm^2 cross-sectional area) (Fig. 1). The
155 cores were cut into 10 cm intervals at the field using a metal spatula and transported to the
156 laboratory under cool, dark conditions. Upon arrival, the cores were immediately air-dried at 60°C

157 until a constant weight was obtained, and bulk density was determined (Kida *et al.*, 2019). The
158 air-dried soil was then passed through a 2 mm mesh size sieve. No gravel was present in any of
159 the samples.

160 In this study, samples from the cores 2, 3, and 5, the deepest of the five cores, were
161 analyzed (Fig. 1). Approximately 5.5 g of the air-dried samples were carefully subsampled using
162 the conical quadrant method to ensure representative subsamples. The samples from a depth of
163 70-94 cm at the point 3 were treated with 2 M HCl overnight to remove inorganic carbon because
164 some shell fragments were visually observed. The treated sample was carefully collected using a
165 metal spoon and analyzed for density fractionation.

166

167 **2.2. Density fractionation**

168 Density fractionation was performed using an aqueous solution of sodium polytungstate
169 (SPT-0, TC-Tungsten Compounds; SPT) with a density of 1.6 g cm^{-3} in accordance with previous
170 studies (Golchin *et al.*, 1994; Wagai *et al.*, 2008). Despite the assumption that SPT produces
171 insoluble precipitates in the presence of calcium ion and thus cannot be used in Ca-rich soils
172 without prior washing, little literature evidence was found to support this argument. In fact, the
173 original support for this notion appeared to be personal communication reported in Six (1999)
174 (Six, 1999). We thus first examined whether marine-derived Ca^{2+} in mangrove soil samples

interferes with the density fractionation experiment using two types of solutions: (1) a filtrate by 0.45μm PTFE membrane filter (Omnipore, Merck) of one of the Fukido mangrove soil samples mixed with deionized water with approximately twice the solid-to-liquid ratio as the density fractionation experiment, and (2) a 0.6 M $CaCl_2$ solution. These solutions were each mixed with the same volume of a 3.2 g cm^{-3} SPT solution, making a 1.6 g cm^{-3} SPT solution with Ca^{2+} concentrations representative of the Fukido samples and unlikely high 0.3 M, respectively. In both cases, no precipitates were found after 24 h. With 0.3 M $CaCl_2$, a small amount of white precipitates (presumably Ca-PT) was observed only after 72h. We thus concluded that a prior desalinating washing step was not necessary for mangrove soils and coastal sediments in general. Omitting the washing step can alleviate the risk of material loss and saves time.

In this study, m-LF was collected through mechanical shaking with glass beads (ϕ 6 mm) at 120 rpm, which facilitated the breakdown of aggregates and detachment of minerals attached to plant residues. We optimized the duration of shaking by comparing m-LF recovery with that obtained through sonication (Fig. 2). Approximately 90% recovery was achieved through 24 h of shaking compared to sonication with a total energy of 120 J mL^{-1} in ice water, which itself showed maximal recovery of m-LF (Fig. 2). The m-LF recovery through shaking also reached a plateau after 24 h, thus this duration was selected for the shaking process.

In density fractionation, five grams of the soil sample was weighed in a 50 mL conical

193 tube and 20 mL of a SPT solution was added, followed by gentle turning over 20 times. The
194 sample was then centrifuged at 700 G for 5 min, and the suspended materials were collected as f-
195 LF using a poly dropper and metal spoon onto a suction filtration device with a 0.45μm PTFE
196 membrane filter (Omnipore, Merck). This procedure was performed three times in total. In order
197 to compensate for the SPT solution lost during the f-LF collection, the SPT solution was
198 replenished every procedure. The collected f-LF was washed three times with 5 mL of 1M KCl
199 to prevent possible inorganic nitrogen contamination from the SPT solution (Rota Wagai, personal
200 communication), rinsed with deionized water until the electrical conductivity (EC) was less than
201 50 μS cm^{-1}, and dried at 80°C for 48 hours. Subsequently, glass beads and the SPT solution were
202 added to the remaining soil, and the sample was shaken reciprocally at 120 rpm for 24 hours. The
203 sample was then centrifuged at 8700 G for 10 min, and the material floating (m-LF) was recovered
204 using the same procedure as the f-LF recovery. Finally, the sample residue in the conical tube
205 (HF) was transferred to a 250 mL centrifuge tube with deionized water, centrifuged at 13000 G
206 for 20 min, and the supernatant was carefully discarded as much as possible using a Komagome
207 pipette. Glass beads were removed with a care not to lose any sample soil after centrifugation.
208 The soil was then treated with 100 mL of 1M KCl (shaken reciprocally for 10 min and centrifuged
209 at 13000 G for 25 min), washed several times with 100 mL of deionized water until the EC reached
210 less than 50 μS cm^{-1}, and freeze-dried. The weight of each fraction was measured and mass

211 recovery was calculated. Using a stereomicroscopy (×20), we observed the morphology of each
212 density fraction. Photographs of representative samples were taken using density samples from
213 another nearby mangrove forest on Ishigaki Island (m-LF collected by sonication) and provided
214 in Fig. 3d because we couldn't take photographs of Fukido samples. The morphological features
215 of the density fractions from these mangroves were almost identical.
216
217 **2.3. Elemental analysis**
218 The elemental composition of bulk soil and each density fraction was determined using
219 an elemental analyzer (PE2400 series II; PerkinElmer). Following grinding and drying at 80 °C
220 for 12 h, the samples were sealed in tin capsules (Tin Capsule Foil, 8 × 5 mm, Exeter Analytical
221 Inc.). Bulk soil and HF fractions were encapsulated in approximately 15 mg, whereas the f-LF
222 and m-LF fractions were encapsulated in approximately 4 mg. Measurements were performed in
223 duplicate and the average value was used for the results. If the coefficient of variation (CV)
224 between two measurements exceeded 10%, a third measurement was performed and the most
225 outlier was removed. The overall analytical precision for C and N was 1.2% and 2.5% by CV,
226 respectively. From the obtained C and N content, the mass recovery of C and N by density
227 fractionation, the contribution of each density fraction to the bulk C and N content, and the C/N
228 ratio were calculated.

2.4. Stable carbon isotope analysis

Stable isotopes of carbon can provide insights into the source of SOM. In mangrove soils, stable carbon isotopes have been used to identify major carbon sources of SOM, patterns of utilization of organic carbon by microbial and animal communities, and to track organic matter exchange between adjacent ecosystems (Bouillon, Connolly, *et al.*, 2008), but never for density fractions. In this study, carbon stable isotope ratios were measured for each density fraction using a continuous flow elemental analyzer/isotope ratio mass spectrometer (EA/IRMS; FLASH EA 1112 series + Thermo Finngan DELTA plus, Thermo Scientific, USA). The carbon stable isotope ratios were expressed in the common delta (δ) notation as the per mil (‰) difference of the $^{13}C/^{12}C$ ratio in a sample relative to the Vienna Pee Dee Belemnite standard. Peach Leaves ($\delta^{13}C$: -26.06‰ ± 0.05‰, NIST1547, Sigma-Aldrich) and Glycine ($\delta^{13}C$: -32.3‰ ± 0.2‰, Aminostandard, Shoko Science) were used as calibration standards. To check the scale-dependent variation of the $\delta^{13}C$ values, the amounts of the standards were varied from 0.03 to 0.07 mg. The calibration curve using the Peach Leaves and Glycine standards was prepared at approximately 0.07 mg and 0.03 mg, respectively, to correct for the deviation of the measured values from the true values of the standard samples. A 5-point calibration with the standards was used to calibrate and normalize the measured isotopic ratios to the international scale. Two standards were run for every 20

247 samples, and 2 blanks and conditioning and calibration standards were included at the beginning
248 and end of each run. Measurement precision and trueness were both within ± 0.14‰ for $\delta^{13}C$ of
249 the laboratory standards.
250
251 **2.5. Radiocarbon analysis**
252 Radiocarbon analysis of density fractions were performed at Yokoyama Lab, AORI,
253 Japan (Yokoyama *et al.*, 2019). We provided approximately 3 mg C for radiocarbon analysis. All
254 samples were sealed in Ag capsules, combusted into CO_2 gas in an elemental analyzer (Vario
255 Micro Cube, Elementar), and converted to graphite by a custom-built graphitization vacuum line
256 (Yokoyama *et al.*, 2022). After graphitization, the radiocarbon content was measured with a
257 single-stage accelerator mass spectrometer (NEC, USA). Radiocarbon data are expressed as ^{14}C
258 ages, percent modern carbon (pMC), and $\Delta^{14}C$ which is the fractional deviation, in parts per
259 thousand (‰), of the sample $^{14}C/^{12}C$ ratio relative to that of the oxalic acid international standard
260 (National Institute of Standards and Technology) (Stuiver and Polach, 1977). Analytical precision
261 for the $\Delta^{14}C$ analysis was better than 4‰.
262
263 **3. Results and Discussion**
264 **3.1. General characteristics and microscopic observations of soil and density fractions**

The evaluation of material recovery is a crucial initial step in reporting the results of density fractionation. Our density fractionation yielded an average soil mass recovery as high as 92.2% (Table 2). The recoveries based on C and N content were also high, albeit slightly lower than those of the mass recovery (Table 2), which are commonly observed in density fractionation analysis of soils. The slight loss could be due to the loss of dissolved matter and fine colloids during the washing step (Wagai *et al.*, 2008). Additionally, a higher loss of N might have resulted from the loss of inorganic N. Overall, these high material recovery rates assured the validity of our approach.

HF was by far the most dominant fraction in the mangrove soils in terms of mass (Fig. 3a). The average mass proportions of f-LF, m-LF, and HF in the bulk soils were 4.9%, 2.9%, and 92.2%, respectively. Yet, the average percentage of the f-LF and m-LF combined (~8%) was higher than that of forest and agricultural soils (Cerli *et al.*, 2012; Crow *et al.*, 2007; Kölbl and Kögel-Knabner, 2004; Parker *et al.*, 2002; Swanston *et al.*, 2005; Wagai *et al.*, 2008). This suggests higher inputs of plant residues such as fine roots and bark fragments and/or their longer residence time in mangrove soils than in upland soils. The amounts of f-LF did not show a clear change with depth and varied largely (Fig. 3a). The m-LF content showed much less variation with depth, but had a notably high value at 30–40 cm in core 3, accompanied by reductions in the C and N concentrations (Fig. 3bc). The HF content was almost constant with depth and between

283 cores. According to stereomicroscopic observation, materials recovered as f-LF were mainly
284 coarse plant residues, with relatively intact mangrove fine roots found in shallower (<50 cm)
285 sections while more fragmented fine roots and bark of coarser roots in deeper sections (still, live
286 fine roots were present in the deepest sections) (Fig. 3d). Much of the plant residues in f-LF was
287 covered with patches of fine mineral particles. In contrast, m-LF looked almost free of mineral
288 particles and consisted of much smaller plant fragments. The use of glass beads and mechanical
289 shaking may have largely broken plant tissues and obscured the morphology. However, m-LF
290 recovered by disruption of aggregates by sonication consisted of similarly small fragments (Fig.
291 3d), thus this fragmented morphology may be a property of m-LF in mangrove soils. As
292 expectedly, HF contained no recognizable plant tissues and was instead dominated by mineral
293 particles (Fig. 3d).

294 The C and N concentrations of the density fractions (Fig. 3bc) were consistent with the
295 microscopic observations. C concentrations were one-order of magnitude higher in LF than in HF,
296 while N concentrations were several times higher. Among LF, m-LF had almost always higher C
297 and N concentrations compared to f-LF (Fig. 3bc). Nitrogen was relatively more enriched (by
298 ~80%) than C (by ~50%) in m-LF than in f-LF, resulting in lower C/N ratios in m-LF (Fig. 5).
299 Higher C and N concentrations in m-LF compared to f-LF have been found in forest and
300 agricultural soils (Wagai et al. 2008 and references there in). Interestingly, only N concentrations

301 showed a clear decline with depth in all fractions (Fig. 3c). This decoupling between C and N
302 dynamics suggests selective consumption or leaching of N-rich compounds and/or selective
303 preservation of C-rich compounds.

304 When evaluating on a bulk soil basis, the C concentrations (mgC g soil^{-1}) in all fractions
305 varied widely and did not show a clear depth trend, while the N concentrations decreased with
306 depth, particularly in the m-LF and HF fractions (Fig. 4ab). The depth distributions of LFs were
307 markedly different from those typically observed in terrestrial soils which tends to decrease
308 rapidly with depth (Luo *et al.*, 2020; Parker *et al.*, 2002; Swanston *et al.*, 2005). This is
309 presumably due to the massive production of mangrove fine roots, even in deep soils. Although
310 data on in-situ fine root production in deep mangrove soils (>30 cm) is scarce, Arnaud et al. (2021)
311 recently showed that a major fraction of fine root production occurs deeper than 30 cm. Other
312 recent papers have also reported fine root production down to a depth of 50–60 cm below ground
313 in mangrove forests (Fujimoto *et al.*, 2021; Ono *et al.*, 2022). Our visual inspection also revealed
314 abundant live and dead fine roots in deep (> 50cm) soils. These results collectively support our
315 first hypothesis. When normalized to the total, f-LF accounted for 14-44% of total soil C and 8-
316 32% of total N, m-LF for 15-36% and 11-23%, and HF for 34-62% and 56-75%, respectively (Fig.
317 4cd). All fractions did not exhibit a clear depth trend, while the variations of %m-LF (CV of 18%
318 and 17% for C and N, respectively) were relatively smaller than that of %f-LF (CV of 28% and

319 39% for C and N, respectively). A recent comprehensive meta-analysis of data obtained by density
320 fractionation of terrestrial soils (n=1222) (Heckman *et al.*, 2022) has revealed that the mean C
321 contribution was 33% for f-LF, 14% for m-LF, and 59% for HF, indicating m-LF is the minimal
322 functional component of SOM in terrestrial soils. Contrarily, our analysis revealed that m-LF was
323 as abundant as f-LF (particularly as N) in the mangrove soils throughout the 1-m cores (Fig. 4cd).
324 The average relative contribution of m-LF carbon in the mangrove soils was 1.6 times higher than
325 that in terrestrial soils (Heckman *et al.*, 2022). In mangrove soils, the longer residence time of
326 plant residues (f-LF, mainly as fine roots) under suboxic conditions may have resulted in greater
327 associations with soil minerals, providing physico-chemical protection for such plant residues
328 from microbial degradation.
329
330 **3.2. Organic matter early diagenesis inferred from C/N ratios and $\delta^{13}C$ values**
331 The C/N ratios of the density fractions showed clear differences between fractions (Fig.
332 5). The C/N ratios of the f-LF, m-LF, and HF ranged from 43.2 to 78.5, 32.0 to 66.8, and 16.8 to
333 33.8, respectively (Fig. 5a). The lower C/N ratio of HF compared to the other low-density
334 fractions is similar to that observed in terrestrial soils, suggesting that microbial degradation of
335 HF was more progressed and that plant-derived components contributed more to the LFs (Liao *et*
336 *al.*, 2006; Tan *et al.*, 2007). There was no obvious difference in $\delta^{13}C$ values between fractions

337 (overall -29.7 to -27.3‰) (Fig. 5b), indicating that the major origin of organic matter differed
338 only little among the fractions. Previous studies have shown that mangrove leaves, microalgae,
339 macroalgae, and seagrasses are important sources of SOM in mangroves (Bouillon, Connolly, *et*
340 *al.*, 2008). Their average $\delta^{13}C$ values are -28.1‰, -20.2‰, -18.9‰, and -12.1‰, respectively
341 (Bouillon, Connolly, *et al.*, 2008), suggesting all fractions were primarily derived from mangroves
342 in the Fukido mangrove forest. The little difference in $\delta^{13}C$ values between density fractions was
343 against commonly observed patterns in terrestrial soils, where organic matter strongly associated
344 with minerals (i.e., HF) is typically enriched in ^{13}C (Sollins *et al.*, 2009), and rejected our second
345 hypothesis.

346 Although there was some variability in f-LF, the C/N ratio clearly increased with depth
347 (Fig. 5a). At the same time, the $\delta^{13}C$ values also showed clear increases with depth, with the
348 exception of f-LF of core 3 (Fig. 5b). The simultaneous increases in the C/N ratios and $\delta^{13}C$ values
349 with depth were against commonly observed patterns in terrestrial soils and not straightforward
350 to interpret. In terrestrial soils under C_3 plants, C/N ratios generally decrease while $\delta^{13}C$ values
351 increase with depth, resulting in a negative correlation between them (Lorenz *et al.*, 2020; Paul *et*
352 *al.*, 2020; Sollins *et al.*, 2009; Werth and Kuzyakov, 2010). However, there are also cases where
353 the carbon-stable isotope ratio decreases with decomposition (Lehmann *et al.*, 2002). Although
354 inorganic carbon can theoretically raise C/N ratios and $\delta^{13}C$ values, we could rule out a

355 contribution from inorganic carbon because the three samples that were subjected to a HCl
356 treatment (70-94 cm at station 3) showed similar C and N concentrations, C/N ratios, and $\delta^{13}C$
357 values compared to the rest of untreated samples (Figs. 2-4). A HCl test on randomly selected
358 samples with no visible inorganic carbon fragments (such as shells or coral fragments) was indeed
359 negative. The reasons for the enrichment in ^{13}C with depth are not yet fully understood, but the
360 ^{13}C enrichment can be the result of temporal changes in the initial composition of C or isotopic
361 effects associated with post-photosynthesis processes in either plants or soils. We summarized
362 possible processes that can affect C/N ratios and $\delta^{13}C$ values of SOM (Table 3). A range of
363 processes is known to influence both parameters in either direction. Among these, only the
364 increased relative dominance of roots compared to leaves could explain the simultaneous
365 increases in the C/N ratios and $\delta^{13}C$ values with depth, although all processes are not mutually
366 exclusive (Table 3). Historical changes in vegetation ^{13}C abundance as a result of changes in
367 atmospheric ^{13}C abundance (^{13}C-Suess effect) (Francey *et al.*, 1999) and/or greater isotopic
368 discrimination during photosynthesis under higher CO_2 levels (Paul *et al.*, 2020) could also
369 explain the increase in $\delta^{13}C$ values with depth (Fig. 5b), but they do not themselves provide an
370 explanation for the increase in C/N ratios (Fig. 5a). The proportion of root-derived C inputs is
371 expected to be higher at depth, and roots generally have higher C/N ratios (by ~5–50) and $\delta^{13}C$
372 values (by ~1–5‰) compared to leaves because of differences in chemical composition and post-

373 photosynthetic allocation mechanisms (Cernusak *et al.*, 2009; Lorenz *et al.*, 2020; Werth and
374 Kuzyakov, 2010; Zeh *et al.*, 2020). In particular, decomposed mangrove roots can exhibit a high
375 C/N ratio. For instance, after one-year of decomposition, mangrove leaves decreased in C/N ratio
376 (from 32 to 18) while roots considerably increased it (from 36 to 66) in a mangrove forest on
377 Pohnpei Island (Ono *et al.*, 2015). In this regard, the decomposition of roots alone might explain
378 the simultaneous increases in the C/N ratios and $\delta^{13}C$ values with depth (Fig. 5b) if ^{13}C kinetic
379 discrimination during microbial utilization favors the enrichment of ^{13}C in residual roots (Ågren
380 *et al.*, 1996; Torn *et al.*, 2002). Previous research has shown that the $\delta^{13}C$ values of mangrove
381 leaves and fine roots in the Fukido mangrove were on average -30.9‰ and -28.7‰, respectively
382 (Fig. 5b), indicating that roots had a heavier carbon isotope signature than leaves (Iimura *et al.*,
383 2019). However, a slight (~1.5‰) but consistent deviation from the simple leaf-to-root mixing
384 model (Fig. 5b) suggests a progressive decreasing input of ^{13}C-enriched materials, such as soil
385 microbial-derived organic matter and marine organic matter, regardless of depth or fractions
386 (Table 3) (Boström *et al.*, 2007; Marchand *et al.*, 2005; Werth and Kuzyakov, 2010). Nonetheless,
387 the marked difference in the C/N ratios between fractions (Fig. 5a) indicates that the density
388 fractions have undergone distinct degradation state and potentially have different ages.

389 Compound-specific C/N ratios of organic compounds in mangrove plants may also
390 explain the observed decline in C/N ratios with depth (Fig. 5a). Selective preservation of phenolic

391 compounds, such as lignin and tannin, in the Fukido River mangrove soils has been reported,
392 based on higher phenolic ^{13}C NMR signals in deeper soils (Kida *et al.*, 2019). Lignin-derived
393 phenols were found to be lost at a lower rate than total neutral sugars and bulk SOM during
394 decomposition in mangrove swamps of French Guiana (Marchand *et al.*, 2005). As lignin lacks
395 N in its chemical structure, its selective preservation would result in an increase in the C/N ratio
396 with depth (Fig. 5a). The increase in C/N ratio in all fractions may suggest that selective
397 preservation of phenolic compounds is occurring in all fractions. Phenolic compounds such as
398 lignin and tannin are organic polymers that undergo a two-step degradation process, first
399 decomposing to small molecules such as phenols, and then mineralization of these small
400 compounds to CO_2. The phenol oxidase involved in the first step requires oxygen as an enzymatic
401 cofactor (Bianchi *et al.*, 2016; Saraswati *et al.*, 2016), making it difficult to occur under reducing
402 conditions in mangrove soils and potentially leading to selective preservation of phenolic
403 compounds (Kida *et al.*, 2019). This selective preservation would lead to the accumulation of
404 persistent phenolic compounds in each fraction, potentially playing a role in carbon storage in
405 mangrove soils. However, selective preservation of lignin would lead to depleted $\delta^{13}C$ values
406 because lignin typically is depleted in ^{13}C compared to other plant constituents such as proteins
407 and cellulose (Bowling *et al.*, 2008). Isotope analysis of plant organic compounds, as well as end-
408 members such as terrestrial, mangrove, and marine sources, could provide further insight into the

409 simultaneous increases in the C/N ratios and $\delta^{13}C$ values with depth (Fig. 5).

410 Finally, isotopic fractionation of dissolved organic carbon (DOC) can also partly
411 account for the $\delta^{13}C$ depth gradient (Bowling *et al.*, 2008; Kaiser *et al.*, 2001). In terrestrial soils,
412 material flow is typically "top-down" due to major organic matter inputs in surface soils and
413 subsequent translocation down to subsurface soils through water flow. This results in increased
414 organic matter age, increased microbial processing, and correspondingly lower C/N ratios with
415 increasing depth (Heckman *et al.*, 2022). During passage through the mineral soil, DOC interacts
416 with the mineral matrix through preferential sorption/desorption of compounds with specific
417 molecular characteristics as in chromatography. These chromatographic behaviors and the decay
418 of labile compounds can alter the isotopic signatures of DOM, and in extension, associated bulk
419 SOM because of differences in $\delta^{13}C$ values among compounds (Bowling *et al.*, 2008). However,
420 the influence of DOC on the isotopic signature of bulk SOM in mangrove soils is unknown, as
421 material flow in these soils is not only vertical, but also horizontal due to organic matter inputs
422 throughout the soil column (~1 m) through massive fine root production (Arnaud *et al.*, 2021;
423 Tabuchi, 1983) and advective translocation of DOC in soils by tidal water movement (Maher *et*
424 *al.*, 2013; Ohtsuka *et al.*, 2020). Therefore, despite the potentially larger role played by DOC in
425 mangrove soils due to water saturation and huge DOC flux, its influences on the isotopic signature
426 of mangrove bulk SOM remain uncertain.

427

428 **3.3. Mineral association as a key factor in long-term carbon storage in mangrove mineral**

429 **soils**

430 The major contribution of m-LF in mangrove soils (Fig. 4) was a novel finding, but its

431 long-term stability needs verification in order for m-LF to be an important fraction for carbon

432 storage in mangrove soils. We therefore conducted a radiocarbon analysis of density fractions in

433 the deepest samples. We found a consistent pattern in $\Delta^{14}C$ values of density fractions in all the

434 measured cores (Table 4). HF was the oldest with $\Delta^{14}C$ between -149‰ and -97‰ followed by

435 m-LF (between -130‰ and -87‰) and then f-LF (between -89‰ and 78‰). These differences in

436 $\Delta^{14}C$ among density fractions were consistent with the findings from terrestrial soils (Heckman

437 *et al.*, 2022) and suggest that mineral association may be pivotal in long-term carbon storage in

438 mangrove mineral soils. In the LFs, m-LF was always older than the corresponding f-LF, although

439 f-LF showed a considerable variability in their $\Delta^{14}C$ (Table 4). The lower $\Delta^{14}C$ values of m-LF

440 indicate that on average, m-LF is more persistent than f-LF. These results suggest that m-LF may

441 play a more important role in carbon storage in mangrove soils than in terrestrial soils. It is likely

442 that slower decomposition under reducing conditions due to flooding resulted in longer residence

443 time of f-LF and greater associations with soil minerals. This is supported by the similar $\Delta^{14}C$

444 values observed for f-LF and m-LF in core 2 (Table 4). The positive $\Delta^{14}C$ (modern age) observed

445 in f-LF of the core 3 was due to recent inputs of live fine roots, while negative $\Delta^{14}C$ values of f-
446 LF in the other cores suggest limited inputs from live roots (Table 4). Questions remain, however,
447 why there are a large variability in $\Delta^{14}C$ between the same fractions of different cores (Table 4).
448 Molecular level analyses of each fraction and more detailed source partitioning by measuring end-
449 members (river, mangrove, and marine) and linking the result to geochemical factors such as
450 specific surface area and reactive metal phases (Fe, Al), may shed light on organic carbon
451 stabilization mechanisms in mangrove soils. A variability in environmental factors such as
452 oxidation-reduction potential, pH, or salinity should simultaneously be considered.
453
454 **4. Conclusion**
455 We introduced density fractionation in mangrove soils in this study. The method could
456 successfully separate meaningful functional components of SOM in mangrove soils which
457 differed in abundance, degradation state, and age. The massive production of mangrove fine roots
458 resulted in a high abundance of plant debris (low-density fractions) throughout the 1-m cores,
459 which markedly differed from terrestrial soils. By analyzing elemental and isotopic signatures of
460 density fractions, we revealed shifts in sources and degradation state within and between fractions.
461 However, although we were able to decipher the important fractions for carbon storage in
462 mangrove soils, the processes generating each density fraction and their influencing factors

remain to be studied. Future studies would benefit from a coupled analysis of quantity (C/N concentrations and relative abundance) and quality (stable and radio isotopes and molecular composition) of density fractions and geochemical factors in the mangrove soil. It is also needed to elucidate how natural environmental variations such as redox conditions and pH influence the association between mineral particles and reactive metal phases and SOM of different nature, on different time scales of hourly, daily, and seasonally over semi-diurnal and spring–neap tidal cycles.

Declarations of interest: none

Contributions: MK designed the experiment and collected the samples with the help of NF. KH conducted the density fractionation experiments with an initial guidance from MK. MK and KH conducted stable isotope analysis with the help of TO. MK, YM, and YY conducted radiocarbon analysis. KH wrote an initial draft with a significant contribution from MK, and all authors have reviewed and approved the final article.

Acknowledgements

This study was supported by JSPS KAKENHI Grant Number 21KK0186 (T.O.) and startup

481 funding from Kobe University (M.K.). We thank Rota Wagai (NIAES/NARO) for his initial
482 guidance in density fractionation.

483

484 **References**

485 Adame MF, Connolly RM, Turschwell MP, *et al.* 2021: Future carbon emissions from global
486 mangrove forest loss. *Glob Chang Biol*, **27**, 2856–2866.

487 Ågren GI, Bosatta E, Balesdent J 1996: Isotope Discrimination during Decomposition of Organic
488 Matter: A Theoretical Analysis. *Soil Science Society of America Journal*, **60**, 1121–1126.

489 Alongi DM 2014: Carbon Cycling and Storage in Mangrove Forests. *Ann Rev Mar Sci*, **6**, 195–
490 219.

491 Arnaud M, Morris PJ, Baird AJ, Dang H, Nguyen TT 2021: Fine root production in a
492 chronosequence of mature reforested mangroves. *New Phytologist*, **232**, 1591–1602.

493 Atwood TB, Connolly RM, Almahasheer H, *et al.* 2017: Global patterns in mangrove soil carbon
494 stocks and losses. *Nat Clim Chang*, **7**, 523–528.

495 Bianchi TS, Schreiner KM, Smith RW, Burdige DJ, Woodard S, Conley DJ 2016: Redox Effects
496 on Organic Matter Storage in Coastal Sediments During the Holocene: A Biomarker/Proxy
497 Perspective. *Annu Rev Earth Planet Sci*, **44**, 295–319.

498 Boström B, Comstedt D, Ekblad A 2007: Isotope fractionation and 13C enrichment in soil profiles

during the decomposition of soil organic matter. *Oecologia*, **153**, 89–98.

Bouillon S, Borges A V., Castañeda-Moya E, *et al.* 2008: Mangrove production and carbon sinks: A revision of global budget estimates. *Global Biogeochem Cycles*, **22**.

Bouillon S, Connolly RodM, Lee ShingY 2008: Organic matter exchange and cycling in mangrove ecosystems: Recent insights from stable isotope studies. *J Sea Res*, **59**, 44–58.

Bowling DR, Pataki DE, Randerson JT 2008: Carbon isotopes in terrestrial ecosystem pools and CO_2 fluxes. *New Phytologist*, **178**, 24–40.

Cerli C, Celi L, Kalbitz K, Guggenberger G, Kaiser K 2012: Separation of light and heavy organic matter fractions in soil — Testing for proper density cut-off and dispersion level. *Geoderma*, **170**, 403–416.

Cernusak LA, Tcherkez G, Keitel C, *et al.* 2009: Why are non-photosynthetic tissues generally 13C enriched compared with leaves in C3 plants? Review and synthesis of current hypotheses. *Functional Plant Biology*, **36**, 199.

Chen C, Hall SJ, Coward E, Thompson A 2020: Iron-mediated organic matter decomposition in humid soils can counteract protection. *Nat Commun*, **11**, 2255.

Crow SE, Swanston CW, Lajtha K, Brooks JR, Keirstead H 2007: Density fractionation of forest soils: methodological questions and interpretation of incubation results and turnover time in an ecosystem context. *Biogeochemistry*, **85**, 69–90.

517 Dicen GP, Navarrete IA, Rallos R V., Salmo SG, Garcia MCA 2019: The role of reactive iron in
518 long-term carbon sequestration in mangrove sediments. *J Soils Sediments*, **19**, 501–510.
519 Dodla SK, Wang JJ, Cook RL 2012: Molecular Composition of Humic Acids from Coastal
520 Wetland Soils along a Salinity Gradient. *Soil Science Society of America Journal*, **76**, 1592–
521 1605.
522 Donato DC, Kauffman JB, Murdiyarso D, Kurnianto S, Stidham M, Kanninen M 2011:
523 Mangroves among the most carbon-rich forests in the tropics. *Nat Geosci*, **4**, 293–297.
524 Francey RJ, Allison CE, Etheridge DM, Trudinger CM, Enting IG, Leuenberger M, Langenfelds
525 RL, Michel E, Steele LP 1999: A 1000-year high precision record of δ^{13} C in atmospheric
526 CO_2. *Tellus B: Chemical and Physical Meteorology*, **51**, 170–193.
527 Fujimoto K, Ono K, Watanabe S, Taniguchi S, Inoue T, Kanayama K, Ogawa T 2021: Estimation
528 of probable annual fine-root production and missing dead roots associated with the ingrowth
529 core method: attempt with major mangrove species on Iriomote Island, southwestern Japan,
530 located in the subtropics. *Mangrove Science*, **12**, 11–24.
531 Golchin A, Oades J, Skjemstad J, Clarke P 1994: Soil structure and carbon cycling. *Soil Research*,
532 **32**, 1043.
533 Hashimoto Y, Hyakumachi M 1998: Effects of vegetation change and soil disturbance on
534 ectomycorrhizas of Betula platyphylla var. japonica: a test using seedlings planted in soils

taken from various sites. *Mycoscience*, **39**.

Heckman K, Hicks Pries CE, Lawrence CR, *et al.* 2022: Beyond bulk: Density fractions explain heterogeneity in global soil carbon abundance and persistence. *Glob Chang Biol*, **28**, 1178–1196.

Huxham M, Langat J, Tamooh F, Kennedy H, Mencuccini M, Skov MW, Kairo J 2010: Decomposition of mangrove roots: Effects of location, nutrients, species identity and mix in a Kenyan forest. *Estuar Coast Shelf Sci*, **88**, 135–142.

Iimura Y, Kinjo K, Kondo M, Ohtsuka T 2019: Soil carbon stocks and their primary origin at mature mangrove ecosystems in the estuary of Fukido River, Ishigaki Island, southwestern Japan. *Soil Sci Plant Nutr*, **65**, 435–443.

Jia B, Niu Z, Wu Y, Kuzyakov Y, Li XG 2020: Waterlogging increases organic carbon decomposition in grassland soils. *Soil Biol Biochem*, **148**, 107927.

Kaiser K, Guggenberger G, Zech W 2001: Isotopic fractionation of dissolved organic carbon in shallow forest soils as affected by sorption. *Eur J Soil Sci*, **52**, 585–597.

Keeling RF, Graven HD, Welp LR, Resplandy L, Bi J, Piper SC, Sun Y, Bollenbacher A, Meijer HAJ 2017: Atmospheric evidence for a global secular increase in carbon isotopic discrimination of land photosynthesis. *Proceedings of the National Academy of Sciences*, **114**, 10361–10366.

553 Keuskamp JA, Schmitt H, Laanbroek HJ, Verhoeven JTA, Hefting MM 2013: Nutrient
554 amendment does not increase mineralisation of sequestered carbon during incubation of a
555 nitrogen limited mangrove soil. *Soil Biol Biochem*, **57**, 822–829.
556 Kida M, Fujitake N 2020: Organic carbon stabilization mechanisms in mangrove soils: A review.
557 *Forests*, **11**.
558 Kida M, Kondo M, Tomotsune M, Kinjo K, Ohtsuka T, Fujitake N 2019: Molecular composition
559 and decomposition stages of organic matter in a mangrove mineral soil with time. *Estuar*
560 *Coast Shelf Sci*, **231**, 106478.
561 Kida M, Tomotsune M, Iimura Y, Kinjo K, Ohtsuka T, Fujitake N 2017: High salinity leads to
562 accumulation of soil organic carbon in mangrove soil. *Chemosphere*, **177**, 51–55.
563 Kida M, Watanabe I, Kinjo K, *et al.* 2021: Organic carbon stock and composition in 3.5-m core
564 mangrove soils (Trat, Thailand). *Science of The Total Environment*, **801**, 149682.
565 Kinjo K, Tokashiki Y, Sato K, Kitou M, Shimo M 2005: Characteristics of Surface Sediments
566 along a Creek in a Mangrove Forest. *Soil Sci Plant Nutr*, **51**, 809–817.
567 Kölbl A, Kögel-Knabner I 2004: Content and composition of free and occluded particulate
568 organic matter in a differently textured arable Cambisol as revealed by solid-state
569 <sup>13<sup> C NMR spectroscopy. *Journal of Plant Nutrition and Soil Science*, **167**, 45–
570 53.

571 Kooner ZS, Jardine PM, Feldman S 1995: Competitive Surface Complexation Reactions of
572 Sulfate and Natural Organic Carbon on Soil. *J Environ Qual*, **24**, 656–662.
573 Kristensen E, Bouillon S, Dittmar T, Marchand C 2008: Organic carbon dynamics in mangrove
574 ecosystems: A review. *Aquat Bot*, **89**, 201–219.
575 Lalonde K, Mucci A, Ouellet A, Gélinas Y 2012: Preservation of organic matter in sediments
576 promoted by iron. *Nature*, **483**, 198–200.
577 Lee C 1992: Controls on organic carbon preservation: The use of stratified water bodies to
578 compare intrinsic rates of decomposition in oxic and anoxic systems. *Geochim Cosmochim*
579 *Acta*, **56**, 3323–3335.
580 Lehmann MF, Bernasconi SM, Barbieri A, McKenzie JA 2002: Preservation of organic matter
581 and alteration of its carbon and nitrogen isotope composition during simulated and in situ
582 early sedimentary diagenesis. *Geochim Cosmochim Acta*, **66**, 3573–3584.
583 Liao JD, Boutton TW, Jastrow JD 2006: Organic matter turnover in soil physical fractions
584 following woody plant invasion of grassland: Evidence from natural 13C and 15N. *Soil Biol*
585 *Biochem*, **38**, 3197–3210.
586 Liu X, Xiong Y, Liao B 2017: Relative contributions of leaf litter and fine roots to soil organic
587 matter accumulation in mangrove forests. *Plant Soil*, **421**, 493–503.
588 Lorenz M, Derrien D, Zeller B, Udelhoven T, Werner W, Thiele-Bruhn S 2020: The linkage of

589 13C and 15N soil depth gradients with C:N and O:C stoichiometry reveals tree species
590 effects on organic matter turnover in soil. *Biogeochemistry*, **151**, 203–220.
591 Lovelock CE, Feller IC, Reef R, Ruess RW 2014: Variable effects of nutrient enrichment on soil
592 respiration in mangrove forests. *Plant Soil*, **379**, 135–148.
593 Luo X, Hou E, Zhang L, Wen D 2020: Soil carbon dynamics in different types of subtropical
594 forests as determined by density fractionation and stable isotope analysis. *For Ecol Manage*,
595 **475**, 118401.
596 Lützow M v., Kögel-Knabner I, Ekschmitt K, Matzner E, Guggenberger G, Marschner B, Flessa
597 H 2006: Stabilization of organic matter in temperate soils: mechanisms and their relevance
598 under different soil conditions - a review. *Eur J Soil Sci*, **57**, 426–445.
599 Maher DT, Santos IR, Golsby-Smith L, Gleeson J, Eyre BD 2013: Groundwater-derived dissolved
600 inorganic and organic carbon exports from a mangrove tidal creek: The missing mangrove
601 carbon sink? *Limnol Oceanogr*, **58**, 475–488.
602 Marchand C, Disnar JR, Lallier-Vergès E, Lottier N 2005: Early diagenesis of carbohydrates and
603 lignin in mangrove sediments subject to variable redox conditions (French Guiana).
604 *Geochim Cosmochim Acta*, **69**, 131–142.
605 Marschner B, Brodowski S, Dreves A, *et al.* 2008: How relevant is recalcitrance for the
606 stabilization of organic matter in soils? *Journal of Plant Nutrition and Soil Science*, **171**,

607 91–110.

608 McKee KL, Cahoon DR, Feller IC 2007: Caribbean mangroves adjust to rising sea level through
609 biotic controls on change in soil elevation. *Global Ecology and Biogeography*, **16**, 545–556.

610 McLeod E, Chmura GL, Bouillon S, Salm R, Björk M, Duarte CM, Lovelock CE, Schlesinger
611 WH, Silliman BR 2011: A blueprint for blue carbon: Toward an improved understanding of
612 the role of vegetated coastal habitats in sequestering CO2. *Front Ecol Environ*, **9**, 552–560.

613 Middleton BA, McKee KL 2001: Degradation of mangrove tissues and implications for peat
614 formation in Belizean island forests. *Journal of Ecology*, **89**, 818–828.

615 Miyajima T, Hori M, Hamaguchi M, Shimabukuro H, Yoshida G 2017: Geophysical constraints
616 for organic carbon sequestration capacity of *Zostera marina* seagrass meadows and
617 surrounding habitats. *Limnol Oceanogr*, **62**, 954–972.

618 Muhammad-Nor SM, Huxham M, Salmon Y, Duddy SJ, Mazars-Simon A, Mencuccini M, Meir
619 P, Jackson G 2019: Exceptionally high mangrove root production rates in the Kelantan Delta,
620 Malaysia; An experimental and comparative study. *For Ecol Manage*, **444**, 214–224.

621 Ohtsuka T, Onishi T, Yoshitake S, *et al.* 2020: Lateral Export of Dissolved Inorganic and Organic
622 Carbon from a Small Mangrove Estuary with Tidal Fluctuation. *Forests*, **11**, 1041.

623 Ohtsuka T, Tomotsune M, Suchewaboripont V, Iimura Y, Kida M, Yoshitake S, Kondo M, Kinjo
624 K 2019: Stand dynamics and aboveground net primary productivity of a mature subtropical

mangrove forest on Ishigaki Island, south-western Japan. *Reg Stud Mar Sci*, **27**.

Ono K, Fujimoto K, Hirata Y, Tabuchi R, Taniguchi S, Furukawa K, Watanabe S, Suwa R, Lihpai S 2022: Estimation of total fine root production using continuous inflow methods in tropical mangrove forest on Pohnpei Island, Micronesia: Fine root necromass accumulation is a substantial contributor to blue carbon stocks. *Ecol Res*, **37**, 33–52.

Ono K, Hiradate S, Morita S, Hiraide M, Hirata Y, Fujimoto K, Tabuchi R, Lihpai S 2015: Assessing the carbon compositions and sources of mangrove peat in a tropical mangrove forest on Pohnpei Island, Federated States of Micronesia. *Geoderma*, **245–246**, 11–20.

Parker JL, Fernandez IJ, Rustad LE, Norton SA 2002: Soil Organic Matter Fractions in Experimental Forested Watersheds. Soil Organic Matter Fractions in Experimental Forested Watersheds. Water, Air, and Soil Pollution.

Paul A, Balesdent J, Hatté C 2020: 13C-14C relations reveal that soil 13C-depth gradient is linked to historical changes in vegetation 13C. *Plant Soil*, **447**, 305–317.

Richards DR, Friess DA 2016: Rates and drivers of mangrove deforestation in Southeast Asia, 2000–2012. *Proceedings of the National Academy of Sciences*, **113**, 344–349.

Riedel T, Zak D, Biester H, Dittmar T 2013: Iron traps terrestrially derived dissolved organic matter at redox interfaces. *Proceedings of the National Academy of Sciences*, **110**, 10101–10105.

643 Romero LM, Smith TJ, Fourqurean JW 2005: Changes in mass and nutrient content of wood
644 during decomposition in a south Florida mangrove forest. *Journal of Ecology*, **93**, 618–631.
645 Santín C, González-Pérez M, Otero XL, Vidal-Torrado P, Macías F, Álvarez MÁ 2008:
646 Characterization of humic substances in salt marsh soils under sea rush (Juncus maritimus).
647 *Estuar Coast Shelf Sci*, **79**, 541–548.
648 Saraswati S, Dunn C, Mitsch WJ, Freeman C 2016: Is peat accumulation in mangrove swamps
649 influenced by the "enzymic latch" mechanism? *Wetl Ecol Manag*, **24**, 641–650.
650 Shields MR, Bianchi TS, Gélinas Y, Allison MA, Twilley RR 2016: Enhanced terrestrial carbon
651 preservation promoted by reactive iron in deltaic sediments. *Geophys Res Lett*, **43**, 1149–
652 1157.
653 Sholkovitz ER 1976: Flocculation of dissolved organic and inorganic matter during the mixing of
654 river water and seawater. *Geochim Cosmochim Acta*, **40**, 831–845.
655 Six J 1999: Recycling of sodium polytungstate used in soil organic matter studies. *Soil Biol*
656 *Biochem*, **31**, 1193–1196.
657 Sollins P, Homann P, Caldwell BA 1996: Stabilization and destabilization of soil organic matter:
658 mechanisms and controls. *Geoderma*, **74**, 65–105.
659 Sollins P, Kramer MG, Swanston C, Lajtha K, Filley T, Aufdenkampe AK, Wagai R, Bowden RD
660 2009: Sequential density fractionation across soils of contrasting mineralogy: Evidence for

both microbial- and mineral-controlled soil organic matter stabilization. *Biogeochemistry*, **96**, 209–231.

Stuiver M, Polach HA 1977: Discussion Reporting of ^{14}C Data. *Radiocarbon*, **19**, 355–363.

Swanston CW, Torn MS, Hanson PJ, Southon JR, Garten CT, Hanlon EM, Ganio L 2005: Initial characterization of processes of soil carbon stabilization using forest stand-level radiocarbon enrichment. *Geoderma*, **128**, 52–62.

Tabuchi ROKASSS 1983: Fine root amount of mangrove forest: A preliminary survey. *Indian Journal of Plant Sciences*, **1**, 31–40.

Tan Z, Lal R, Owens L, Izaurraralde R 2007: Distribution of light and heavy fractions of soil organic carbon as related to land use and tillage practice. *Soil Tillage Res*, **92**, 53–59.

Torn MS, Lapenis AG, Timofeev A, Fischer ML, Babikov B V., Harden JW 2002: Organic carbon and carbon isotopes in modern and 100-year-old-soil archives of the Russian steppe. *Glob Chang Biol*, **8**, 941–953.

Wagai R, Mayer LM, Kitayama K 2009: Nature of the "occluded" low-density fraction in soil organic matter studies: A critical review. *Soil Sci Plant Nutr*, **55**, 13–25.

Wagai R, Mayer LM, Kitayama K, Knicker H 2008: Climate and parent material controls on organic matter storage in surface soils: A three-pool, density-separation approach. *Geoderma*, **147**, 23–33.

679 Werth M, Kuzyakov Y 2010: 13C fractionation at the root–microorganisms–soil interface: A
680 review and outlook for partitioning studies. *Soil Biol Biochem*, **42**, 1372–1384.
681 Yarwood SA 2018: The role of wetland microorganisms in plant-litter decomposition and soil
682 organic matter formation: a critical review. *FEMS Microbiol Ecol*, **94**.
683 Yokoyama Y, Miyairi Y, Aze T, *et al.* 2019: A single stage Accelerator Mass Spectrometry at the
684 Atmosphere and Ocean Research Institute, The University of Tokyo. *Nucl Instrum Methods*
685 *Phys Res B*, **455**, 311–316.
686 Yokoyama Y, Miyairi Y, Aze T, *et al.* 2022: Efficient radiocarbon measurements on marine and
687 terrestrial samples with single stage Accelerator Mass Spectrometry at the Atmosphere and
688 Ocean Research Institute, University of Tokyo. *Nucl Instrum Methods Phys Res B*, **532**, 62–
689 67.
690 Zeh L, Igel MT, Schellekens J, Limpens J, Bragazza L, Kalbitz K 2020: Vascular plants affect
691 properties and decomposition of moss-dominated peat, particularly at elevated temperatures.
692 *Biogeosciences*, **17**, 4797–4813.
693 Zhang Y, Du J, Ding X, Zhang F 2016: Comparison study of sedimentary humic substances
694 isolated from contrasting coastal marine environments by chemical and spectroscopic
695 analysis. *Environ Earth Sci*, **75**, 378.
696 Zhao B, Yao P, Bianchi TS, Shields MR, Cui XQ, Zhang XW, Huang XY, Schröeder C, Zhao J,

697 Yu ZG 2018: The Role of Reactive Iron in the Preservation of Terrestrial Organic Carbon in
698 Estuarine Sediments. *J Geophys Res Biogeosci*, **123**, 3556–3569.
699

700 **Table 1.** Mechanisms that contribute to stabilization of soil organic matter (SOM) in coastal vegetated soils and evidence for and against each mechanism.

701

Mechanisms	Evidence	References	Counter-evidence	References
Reducing condition	● Kinetic limitation of lignin degradation (”Enzyme-latch”) ● Millennial-scale stability of mangrove peat	McKee et al., 2007; Saraswati et al., 2016	● Variable relationships between saturation conditions and OM decomposition rates ● Leaching of water-soluble compounds ● Iron-mediated organic matter decomposition ● Iron dissolution and decline in physicochemical protection	Chen et al., 2020; Huxham et al., 2010; Romero et al., 2005
Recalcitrance of roots	● Relative preservation of roots compared to leaves	Liu et al., 2017; Middleton and McKee, 2001	● Only explains at most ~10s-years persistence	Same references as the left
Nutrient limitation	● Enhanced decomposition by nutrient enrichment	Huxham et al., 2010	● Variable effects of nutrient enrichment	Keuskamp et al., 2013; Lovelock et al., 2014
Physical protection by minerals	● Iron accumulation around root wall ● Coaggregation of OM and Fe at the redox interface ● Correlation between clay and OM content ● Correlation with specific surface area of sediment	Miyajima et al., 2017; Riedel et al., 2013; Yarwood, 2018	● No relationship between clay and OM content	Kida et al., 2021
Chemical interaction with minerals	● Association between OM and active Fe in coastal sediments via ligand exchange	Dicen et al., 2019; Lalonde et al., 2012; Shields et al., 2016	● Competition between SO_4^{2-} and OM during ligand exchange ● Iron-mediated organic matter decomposition ● Iron dissolution and decline in physicochemical protection	Chen et al., 2020; Jia et al., 2020; Kooner et al., 1995
Salinity-induced immobilization	● Flocculation of dissolved OM at the estuary ● Mobilization of SOM by reduction in salinity	Kida et al., 2017; Sholkovitz, 1976	?	

Table 2. Mass recovery rate and weight recovery rate of C and N relative to the mass.

Core	Mass recovery (%)	C recovery (%)	N recovery (%)
2	92.6±1.0	85.2±12.5	81.8±8.1
3	92.4±1.5	89.6±11.9	83.8±6.7
5	91.7±2.0	97.0±8.5	86.6±4.4

Table 3. Processes that can change C/N ratios and $\delta^{13}C$ values of soil organic matter under C_3 plants. The direction of change is expressed as downward change in a soil column.

Processes	Downward change in a soil column		References
	C/N ratio	$\delta^{13}C$ value	
Dominance of roots compared to shoots/leaves	increase	increase	Werth and Kuzyakov, 2010; Zeh et al., 2020
Selective preservation of lignin	increase	decrease	Bowling et al., 2008; Kida et al., 2019
^{13}C kinetic discrimination during microbial utilization	-	variable†	Ågren et al., 1996; Torn et al., 2002; Werth and Kuzyakov, 2010
Increased contribution from soil microbial-derived organic matter	decrease	increase	Boström et al., 2007; Werth and Kuzyakov, 2010
Increased contribution from marine organic matter	decrease	increase	Bouillon et al., 2008b
Historical changes in atmospheric ^{13}C abundance (^{13}C-Suess effect)	-	increase	Francey et al., 1999
Greater isotopic discrimination during photosynthesis under higher CO_2 levels and associated historical changes in vegetation ^{13}C abundance	-	increase	Keeling et al., 2017; Paul et al., 2020

† Microbial utilization generally results in ^{13}C enrichment in residual substrates but see a review by Werth and Kuzyakov (2010).

709 **Table 4.** Radiocarbon (± 1σ) of the density fractions of Fukido mangrove soil cores. The numbers
710 after "FUK" represent the soil core numbers and depths of the sections analyzed.

Lab code	Sample name	Depth (cm)	^{14}C age (yr BP)	pMC (%)	Δ^{14}C (‰)
YAUT-081125	FUK_2_90_f-LF	80–90	637 ± 20	92.37 ± 0.23	-84.40 ± 2.23
YAUT-079333	FUK_2_90_m-LF	80–90	662 ± 32	92.09 ± 0.37	-87.04 ± 3.65
YAUT-080338	FUK_2_90_HF	80–90	747 ± 24	91.12 ± 0.27	-96.86 ± 2.68
YAUT-079336	FUK_3_94_f-LF	90–94	modern	108.75 ± 0.41	78.02 ± 4.08
YAUT-079337	FUK_3_94_m-LF	90–94	1051 ± 32	87.74 ± 0.35	-130.23 ± 3.48
YAUT-081124	FUK_3_94_HF	90–94	1222 ± 19	85.89 ± 0.20	-148.66 ± 2.01
YAUT-080339	FUK_5_90_f-LF	80–90	678 ± 20	91.90 ± 0.23	-89.07 ± 2.32
YAUT-079338	FUK_5_90_m-LF	80–90	827 ± 31	90.22 ± 0.35	-105.65 ± 3.47
YAUT-079339	FUK_5_90_HF	80–90	984 ± 29	88.47 ± 0.32	-122.97 ± 3.15

711

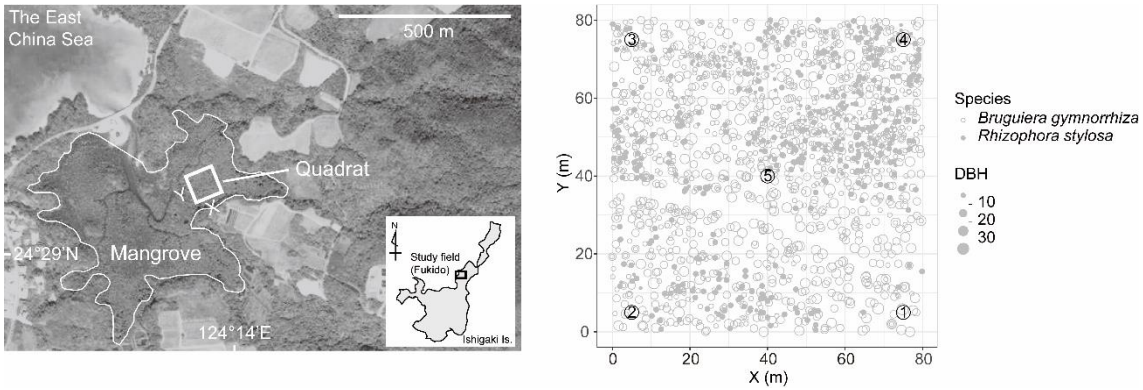

712 **(Two-column figure)**

713 **Fig. 1** Map of the Fukido River mangrove forest site. The white square in the left panel indicates the
714 80 m × 80 m permanent quadrat, while the right panel shows the quadrat with sampling points denoted
715 with numbers. DBH = diameter (in cm) at breast height

716

717

718

719

720

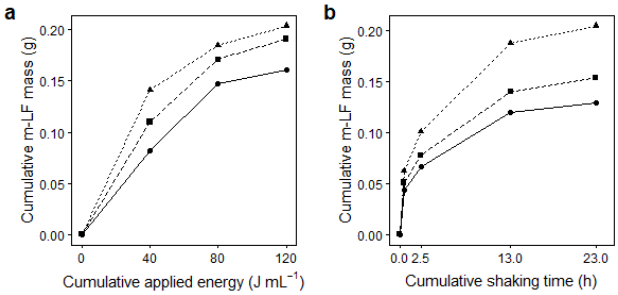

721

722 **(One-column figure)**

723 **Fig. 2** Comparison of mineral-associated low-density fraction (m-LF) recovery by sonication (a) and
724 mechanical shaking (b). Surface, medium, bottom samples of the core 3from the Fukido mangrove
725 soils used in the study were tested, where the corresponding line types in (a) and (b) represent the
726 identical samples

727

728

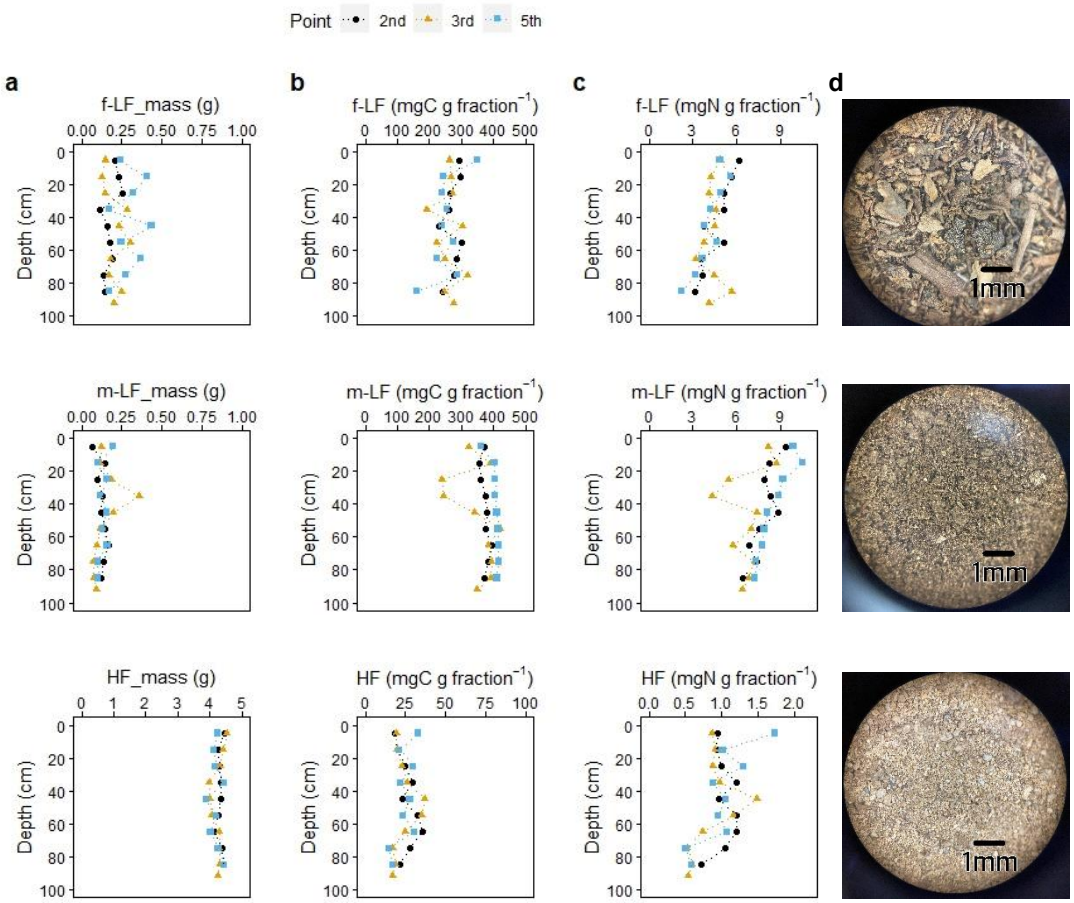

(Two-column figure)

Fig. 3 Contribution of each density fraction to total soil mass (partitioned from 5 g) (a) and C and N concentrations of each fraction on fraction basis (b, c) with depth. The stereomicroscopic photographs of representative samples of each fraction are also provided in (d). Note the different x-scale between fractions. In (a), the x-axis of f-LF and m-LF was magnified by a factor of five compared to that of HF, while in (b) and (c), the x-axis of HF was magnified by a factor of five. f-LF: free low-density fraction, m-LF: mineral-associated low-density fraction, and HF: high-density fraction

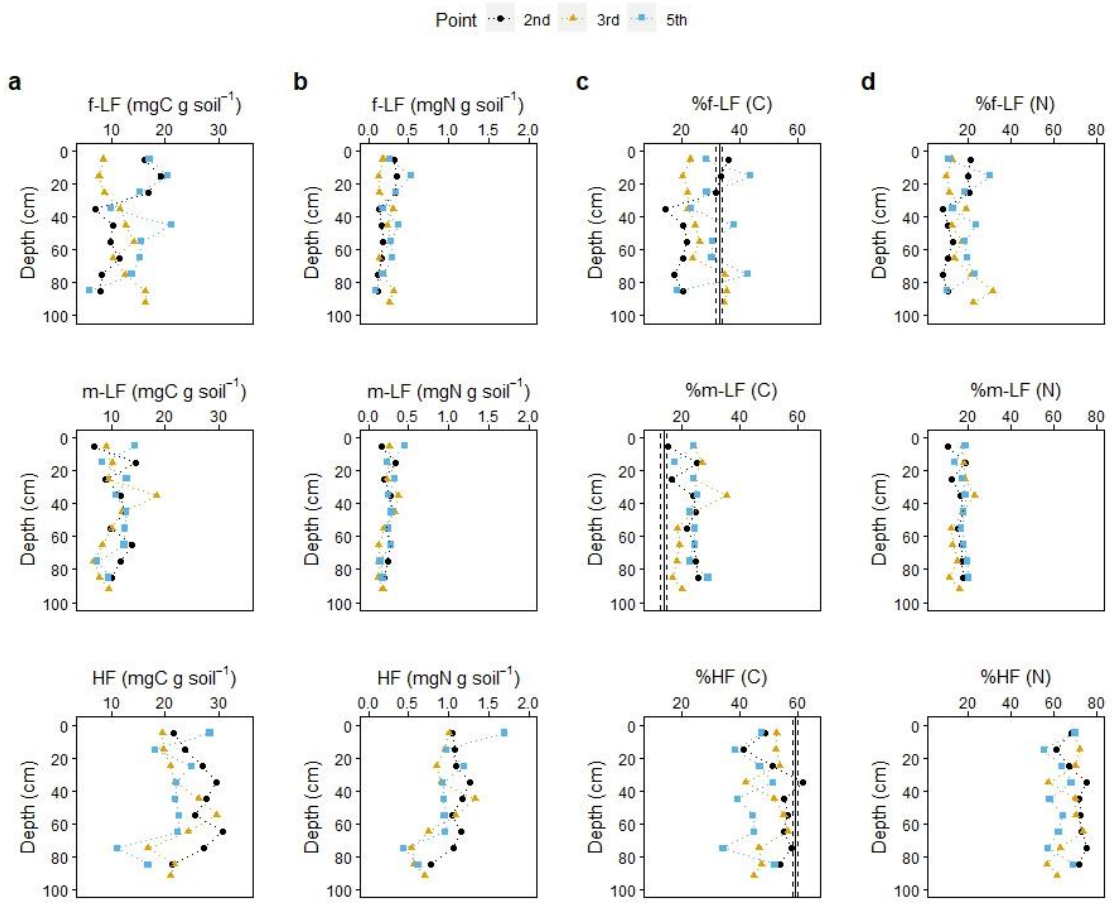

764

765 **(Two-column figure)**

766 **Fig. 4** Contribution of each density fraction to total soil C (a, c) and N (b, d) content with depth.
767 Results are presented in C and N concentrations of each fraction on bulk soil basis (a, b) and relative
768 abundance of each fraction in bulk C and N abundance (c, d). The vertical lines in (C) represent means
769 (solid line) and one standard errors (dashed line) of the relative abundance of density fractions in 1222
770 terrestrial soils reported by Heckman et al. (2022). f-LF: free low-density fraction, m-LF: mineral-
771 associated low-density fraction, and HF: high-density fraction

772

773

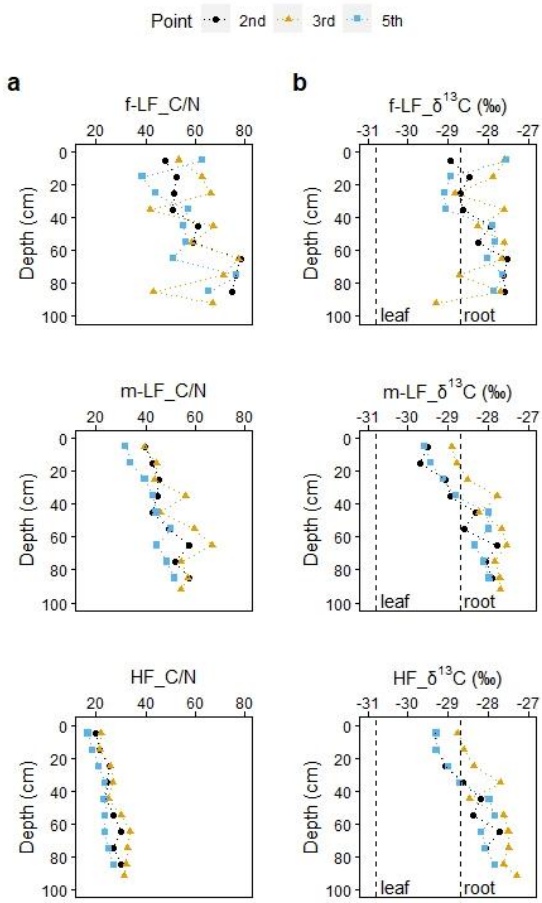

(One-column figure)

Fig. 5 C/N ratio and $\delta^{13}C$ stable isotope ratio of each fraction with depth. f-LF: free low-density fraction, m-LF: mineral-associated low-density fraction, and HF: high-density fraction. The vertical dashed lines in the $\delta^{13}C$ results represent the average $\delta^{13}C$ values for leaf and root of mangroves in the Fukido mangrove forest reported by Iimura et al., 2019